High Frequency Anodising of Aluminium-TiO2 Surface Composites

Anodising Behaviour and Optical Appearance

Gudla, Visweswara Chakravarthy; Bordo, Kirill; Jensen, Flemming; Canulescu, Stela; Yuksel, Serkan; Simar, Aude; Ambat, Rajan

Published in:
Surface and Coatings Technology

Link to article, DOI:
10.1016/j.surfcoat.2015.07.035
10.1016/j.surfcoat.2015.07.035

Publication date:
2015

Document Version
Peer reviewed version

High Frequency Anodising of Aluminium-TiO_2 Surface Composites: Anodising Behaviour and Optical Appearance

Visweswara Chakravarthy Gudla, Kirill Bordo, Flemming Jensen, Stela Canulescu, Serkan Yuksel, Aude Simar, Rajan Ambat

PII: S0257-8972(15)30143-2
DOI: doi: 10.1016/j.surfcoat.2015.07.035
Reference: SCT 20409

To appear in: *Surface & Coatings Technology*

Received date: 13 June 2015
Revised date: 15 July 2015
Accepted date: 17 July 2015

Please cite this article as: Visweswara Chakravarthy Gudla, Kirill Bordo, Flemming Jensen, Stela Canulescu, Serkan Yuksel, Aude Simar, Rajan Ambat, High Frequency Anodising of Aluminium-TiO_2 Surface Composites: Anodising Behaviour and Optical Appearance, *Surface & Coatings Technology* (2015), doi: 10.1016/j.surfcoat.2015.07.035

High Frequency Anodising of Aluminium-TiO_2 Surface Composites: Anodising Behaviour and Optical Appearance

Visweswara Chakravarthy Gudla,[a,*] Kirill Bordo,[a] Flemming Jensen,[a,b] Stela Canulescu,[c] Serkan Yuksel,[a] Aude Simar[d] and Rajan Ambat[a]

[a]*Department of Mechanical Engineering, Technical University of Denmark, Produktionstorvet, DK-2800 Kgs. Lyngby, Denmark*

[b]*Bang & Olufsen A/S, Peter Bangs Vej 15, DK-7600 Struer, Denmark*

[c]*Department of Photonics Engineering, Technical University of Denmark, Frederiksborgvej 399, DK-4000 Roskilde, Denmark*

[d]*iMMC, Université catholique de Louvain, Place Sainte Barbe 2, 1348 Louvain-la-Neuve, Belgium*

**Corresponding author - vichg@mek.dtu.dk, chakri_gvc@yahoo.co.in (Tel: +45-45252118, Fax: +45-45936213)*

Abstract

High frequency anodising of Al-TiO_2 surface composites using pulse reverse pulse technique was investigated with an aim to understand the effect of the anodising parameters on the optical appearance, microstructure, hardness and growth rate of the anodic layer. Friction stir processing was employed to prepare the Al-TiO_2 surface composites, which were anodised in a 20 wt.% sulphuric acid bath at 10 °C as a function of pulse frequency, pulse duty cycle, and anodic cycle voltage amplitudes. The optical appearance of the films was characterized and quantified using an integrating sphere-spectrometer setup, which measures the total and diffuse reflectance from the

surface. The change in optical reflectance spectra from the anodised layer was correlated to the applied anodising parameters and microstructure of the anodic layer as well as the Al-TiO_2 substrate. Change in hardness of the anodised layer was also measured as a function of various anodising parameters. Anodic film growth, hardness, and total reflectance of the surface were found to be highly dependent on the anodising frequency and the anodic cycle potential. Longer exposure times to the anodising electrolyte at lower growth rates resulted in lowering of the reflectance due to TiO_2 particle degradation and low hardness due to increased dissolution of the anodised layer during the process.

Keywords: High Frequency Anodising; Aluminum-TiO_2 Surface Composite; Microstructure; Hardness; Reflectance; TEM.

1. Introduction

Anodising of aluminium is widely used in different fields of industry for corrosion protection, wear resistance, and appealing decorative/cosmetic appearances [1][2]. Decorative anodised surfaces are commonly produced by direct current (DC) anodising of aluminium in a sulphuric acid bath [3]. The resulting anodic alumina layers are usually transparent to the visible light; however, their optical appearance depends on the anodising parameters as well as on the composition and surface morphology of the specimen being anodised [4][5]. White appearing anodised Al surfaces have found applications in the aerospace industry for their high solar reflectance [6][7]. Gudla et.al [8] have shown that different kinds of light-grey to white appearance can be obtained by introducing the metal oxide particles into the Al matrix and further anodising the Al-metal oxide surface composite. The reflectance values obtained were highly dependent on the microstructural aspects of the anodic layer resulting from the differences in anodising parameters[9]. It was shown that the presence of un-anodised Al in the anodic alumina matrix can result in absorption of light resulting in reduced reflectance from the anodised surfaces [10][11][12].

Recently high-frequency anodising of cast Al-Si alloys containing primary Si phases was reported [13]. The microstructure of the obtained porous anodic films is different compared to the anodic layers produced by conventional DC anodising [14]. In particular, the high frequency anodising was accompanied by branching of the anodic pores and effective oxidation of the Al below the primary Si phases [15]. Applying the technique of high frequency anodising to Al-TiO_2 surface composites is expected to completely oxidize the Al phase (which absorbs light in anodic layer) surrounding the TiO_2 particles and improve the reflectance of the resulting anodised surfaces.

Friction stir processing (FSP) [16][17] is a rapid solid state processing technique, which has been extensively used for preparation of various types of surface composites. The objective of the present work is to study the high frequency anodising of FSP surface composites of Al-TiO_2 and to determine the effect of the anodising parameters on the growth behaviour, surface reflectance, microstructure, and hardness of the anodic films. The TiO_2 particles were used to prepare the Al-TiO_2 surface composites via friction stir processing. Rutile form of TiO_2 was chosen for its high refractive index compared to the anodic alumina [18]. Average particle size of 210 nm was chosen for optimum scattering efficiency [19]. Integrating sphere setup was used for characterising the surface reflectance and high resolution SEM and TEM were employed to observe the anodised layers structure.

2. Experimental

2.1 Composites and Surface Preparation

Aluminium substrates with dimensions of 200 x 60 x 6 mm were obtained in rolled condition and commercial powders of TiO_2 (Ti-Pure, DuPont R900, Rutile, D_{50}= 210 nm) were used. The Friction stir processing (FSP) was performed using a Hermle milling machine equipped with a steel tool having 20 mm shoulder diameter, 1.5 mm pin length with a M6 thread, and three flats. The TiO_2 powder is placed in grooves and the friction stir process distributes it in the aluminium surface. The friction stir processing resulted in a Al-TiO_2 surface composite with approx. 2.3 wt.% TiO_2, more details are presented elsewhere [9]. The processed surface composites were initially subjected to rough grinding using an abrasive wheel to remove the flash formed during the FSP process. This was followed by polishing using an abrasive alumina paste of different

size grades (finest size of the abrasive in the last step was 1 µm). The surfaces were then fine polished to a mirror finish using a soft polishing disc. The polished surfaces were subsequently degreased in a mild alkaline solution (30 g/l, Alficlean™, Alufinish, Germany). Desmutting was performed by immersing in a 100 g/l HNO_3 solution followed by demineralised water rinsing. Finally the samples were cleaned by ultra-sonication in acetone for 15 min and dried in air flow.

2.2 High Frequency Anodising

Figure 1

The FSP surface composites were then anodised in a 20 wt.% sulphuric acid bath maintained at 10 °C. Anodising was performed by applying square voltage pulses from a function generator (33120A, Agilent) as shown in Figure 1. The waveforms of voltage and current during the anodising were monitored with the help of a digital oscilloscope (TDS3034B, Tektronix). The anodised area was approximately 2 cm^2. The potential at the cathodic cycle was -2 V (low voltage cycle, V_2), while the potential during the anodic cycle was either +10 V or +20 V (high voltage cycle, V_1). The pulse frequency was varied between 0.1 kHz and 10 kHz. The duty cycle (i.e. the ratio between the anodic cycle duration, t_1 and the time interval between two subsequent pulses, $t_1 + t_2$ was 30 %, 50 % or 70 %. The total anodising time was varied for each set of anodising parameters in order to achieve an anodic layer thickness of approx. 12 µm. The thickness of the obtained anodic layers was measured using a capacitance probe (Omniprobe, Fischer) with a precision of 1 µm.

2.3 Optical Appearance

Surface appearance of the FSP surface composites after anodising was analysed using an integrating sphere-spectrometer setup. The samples were illuminated with white light from a deuterium tungsten halogen light source (DH-2000, Ocean Optics). Reflected light from the samples was collected using an integrating sphere and analysed for diffuse and total reflectance with a fibre optic spectrometer (QE65000, Ocean Optics) in the wavelength range from 300 nm to 750 nm. The spectrometer was calibrated using NIST standards.

2.4 Microstructural Characterization

The microstructure and surface morphology of the obtained anodic layers were studied using SEM (Quanta 200 ESEM FEG, FEI) having EDS capability (80 mm^2 X-Max silicon drift detector, Oxford Instruments). The SEM was typically operated at an acceleration voltage of 10 keV. For cross-sectional imaging, the samples were machined through thickness, mounted in an epoxy and mechanically polished. In order to minimize charging, the samples were coated by a 2-3 nm Au layer by magnetron sputtering (Cressington 208HR sputter coater). Transmission electron microscopy was employed to obtain high resolution images of the anodic layer cross-sections. A TEM (Tecnai G2 20), operating at 200 keV was used for generating bright field images. The sample lamella from the anodised surfaces were prepared using in-situ focused ion beam lift out and subsequent thinning using FIB-SEM (Helios Nanolab Dualbeam, FEI). The micro-Vickers hardness of the anodised surfaces was measured using a Future-Tech FM 700 micro-hardness tester with a load of 10 g – 25 g for 5 s. For each sample, a minimum of 20 measurements were performed to get a reliable average value.

3. Results and Discussion

3.1 Rate of the anodic film growth

The growth of anodic films on FSP-treated surface composite layer was found to be strongly dependent on the anodising conditions, namely the anodic cycle potential and the pulse frequency. Figure 2 shows the effect of the anodic cycle potential, pulse frequency, and duty cycle on the rate of anodic film growth. Increasing the pulse frequency from 0.1 kHz to 10 kHz leads to a significant increase in the growth rate across all duty cycles (Figure 2 (a)). The growth rate increases rapidly up to a frequency of 2 kHz, while from 2 to 10 kHz the increase in the growth rate is less significant. Further, the anodic growth rate is high for higher anodic cycle potential values. When the anodic cycle voltage increases from +10 V to +20 V, the growth rate increases from 0.9 μm/min to 2.1 μm/min at an anodising frequency of 2 kHz. On the other hand, changing the duty cycle does not show any notable effect on the growth rate (Figure 2 (b)) at lower anodic cycle potential values (+10 V). A mixed dependence on duty cycle is observed for higher anodic cycle potential values (+20 V).

Further, the rate of anodic film growth for high-frequency pulse reverse pulse anodising of FSP surface composites was found to be significantly higher than that for conventional DC anodising at the same value of anodic potential. For example, pulse reverse pulse anodising of the composite surfaces at 2 kHz and at an anodic potential of +10 V proceeds at a rate at least 2 times higher than DC anodising at +10 V for pure Al [1][2]. Therefore, the high-frequency anodising can be advantageous for surface composites compared to the conventional DC anodising when thick anodic layer coatings are required.

Figure 2

Kanagaraj et al. [20] have reported that the thickness of the anodic layer increased for a given anodising time by increasing the pulse frequency from 0.01 Hz to 100 Hz. Similarly, increasing the duty cycle or the anodising current density also resulted in increased anodic layer thickness. This increase in anodic growth rate and better quality of anodic films was attributed to the amount of time allowed for the dissipation of heat, which is generated during anodising cycle. The optimum duty cycle for best anodic film properties on AA1100 was stated as 75 % - 80 %, but the corresponding pulse frequency was not reported [21]. Inferior properties measured on the anodic films obtained above this duty cycle level was attributed to the higher heat generated during longer anodic pulse cycle and subsequent lower 'off' time that does not allow effective heat dissipation. However, a clear explanation and correlation between the heat dissipation and anodic film growth rate was not reported. Yokoyama et al. [22] in their initial studies on advantages of pulse anodising emphasize that the recovery effect (chemical dissolution of anodic oxide) during the low voltage cycle or the 'off' cycle will enhance the rate of anodic film growth. However, the pulse frequencies in those studies were lower than 100 Hz.

In the current work, the positive effect of increasing pulse frequency on the anodising growth rate could signify the contribution of recovery effect and also the heat dissipation during the cathodic cycle. However, too low cathodic cycle period (50 μs at 10 kHz) will be insufficient for the recovery to take place due to negligible dissolution of the anodic oxide [23]. Therefore, the observed higher growth rates can be attributed to the lower heat generation during the short anodic cycle and the effective dissipation of this heat during the cathodic cycle.

The weak dependence of anodic growth rate on the duty cycle at +10 V anodic cycle potential shows that the effect of 'off' time or cathodic cycle time is minimal. One can speculate that the heat generated during the anodic cycle is effectively removed during the subsequent cathodic cycle for all duty cycles investigated. Also, the higher growth rates observed for higher anodic cycle potential values result in the observed differences in duty cycle dependence for +10 V and +20 V anodic cycle potential. However, additional investigations are necessary to fully elucidate the effect of high frequency pulse anodising of Al-TiO_2 surface composites and the effect of duty cycle.

3.2 Microstructure and Morphology

The representative microstructure and morphology of the anodic layers obtained after high frequency anodising using +10 V as anodic cycle potential is shown in Figure 3. The SEM-BSE images show that the particles are uniformly dispersed in the Al matrix and similarly are uniformly incorporated into the anodic layer after anodising. There is an observable difference in the contrast from the TiO_2 particles at the top half of the anodised layer when compared to the bottom half close to the Al-TiO_2 substrate interface (see Figure 3 (a)). Moreover, high magnification image in Figure 3 (b) also shows a contrast within the TiO_2 particles in the anodic layer. This difference in contrast in back scatter detection mode was shown to be due to localised transformation in the morphology of the individual TiO_2 particles [9].

Figure 3

Bright field TEM images (see Figure 3 (c) and (d)) of the anodic layer cross sections show change in morphology of the TiO_2 particles from crystalline to porous-amorphous phase, and hence they appear darker in the SEM-BSE images. In some cases, voids are present at TiO_2 particle locations. A closer look shows an associated change in the structure of the anodic pores at the TiO_2 particle locations. Figure 3 (d) shows 'pore branching' in the anodic layer and at the anodic layer-Al metal interfaces, and the anodic pores preferentially grow more inwards into the substrate. This could be due to the ease of access for the anodising electrolyte at the locations where TiO_2 particles have changed their morphology.

Figure 4

The structure of the anodic layers obtained after anodising with an anodic cycle potential of +20 V is shown in Figure 4. Features that were observed in Figure 3 for the + 10 V anodic cycle potential can also be seen here. The dark appearance of the TiO_2 particles in this case extends throughout the anodic layer thickness (see Figure 4 (a)). Also, there is no difference in contrast within the TiO_2 particles in the anodic layer (see Figure 4 (b)). Bright field TEM image confirms that the TiO_2 particles are completely transformed in morphology to porous-amorphous phase (Figure 4 (c)), and also shows the presence of voids at TiO_2 particle locations. High magnification image of the anodic layer-Al substrate interface shows a TiO_2 particle situated at the interface showing porous nature for the region in the anodic layer and a remnant dense crystalline TiO_2 in the Al substrate (see Figure 4 (d)).

Summarising the observations from Figure 3 and Figure 4, it is clear that the increase in anodic cycle potential from +10 V to + 20 V increases the fraction of structurally transformed TiO_2 particles from crystalline rutile phase to amorphous phase. The presence of voids at TiO_2 particle

locations can be due to two factors: (i) the particles may have been completely transformed, i.e. dissolved, and subsequently lost into the anodising electrolyte, or (ii) they are loosely bound to the matrix so that it is lost during the mechanical preparation of the cross sections of the samples. However, from the reflectance spectra shown in Figure 6, at a wavelength of 300 nm - 350 nm, the absorption edge of TiO_2 still exists for both the samples [24][25]. This implies that the surfaces generated at +10 V and at +20 V anodic cycle potentials contain incorporated TiO_2 in the anodic layer, ruling out the loss of TiO_2 into the anodising electrolyte under the anodising conditions. The pore branching observed at TiO_2 particle locations is more severe in the case of +10 V than compared to +20 V. A detailed analysis of the generation of these microstructures and observed features in the morphology of the high frequency anodised FSP surface composite surfaces was recently reported by Gudla et al. [26]. The specific features of pore branching was explained to be due to the increased conductivity of the oxygen deficient TiO_2 under the high frequency pulse reverse pulse conditions. This results in current localisation during the cathodic cycle at the particle locations leading to the localised pore branching.

3.3 Reflectance measurements

Figure 5

Optical reflectance of the anodised FSP composite surfaces was measured as a function of anodic layer thickness, anodic cycle potential, and pulse frequency. Figure 5 shows the effect of the anodic layer thickness on the optical reflectance. Overall the total and diffuse reflectance showed decreasing trend with increasing anodic layer thickness. This is expected since the light absorption increases with the thickness of the anodic oxide layer. At higher anodic layer thicknesses (approx.

23 μm and 36 μm), the reflectance values show a high dependence on the wavelength. The total and diffuse reflectance values observed are lower at lower wavelengths and gradually increase with increasing wavelength. However, the wavelength dependence is less pronounced at lower anodic layer thicknesses.

Figure 6

The reflectance spectra in Figure 6 shows that the increasing potential in the anodic cycle from +10 V to +20 V (at 2 kHz frequency, 50 % duty cycle) leads to an increase in both the diffuse and total reflectance. The total reflectance of the samples in the visible range also increases monotonically with the increase in the pulse frequency from 0.1 kHz to 10 kHz (see Figure 7 (a)) for a given anodic layer thickness at +10 V anodic cycle potential. However, this dependence on anodising frequency is almost negligible when the anodic cycle potential is increased to +20 V (see Figure 7(b)) and the maximum reflectance observed is approx. 60 % (at 10 kHz frequency) for both the surfaces. The wavelength dependence of reflectance is less pronounced with increase in anodic cycle voltage or with increase in pulse frequency compared to results for thicker films (Figure 5). Although not shown here, duty cycle did not show significant effect on reflectance.

Figure 7

The reflectance spectra of the high frequency anodised samples (see Figure 6) show increasing reflectance with increasing anodic cycle potential. The anodised layers contain light scattering TiO_2 particles in either partially crystalline and/or completely amorphous phase as seen from the SEM and TEM images (see Figure 3and Figure 4). The refractive index for crystalline

phase TiO_2 is higher than the amorphous phase and hence better light scattering is expected where partial crystallinity is still maintained for TiO_2 particles in the anodic layer. This implies that better reflectance should be observed for samples anodised at +10 V compared to +20 V. As this is not the case, the lower reflectance for +10 V anodised surface might be arising from other factors such as the presence of light absorbing phases in the anodic layer. It has been previously reported that the presence of un-anodised metallic phases in the anodic layer leads to absorption of light and darkening of the anodised surfaces [11][12][27][28][29]. Anodising at low voltage results in a large fraction of incomplete anodising of Al leading to more pronounced absorption of light and lower reflectance values[9][10]. Also, for TiO_2 containing DC anodised layers, anodising at lower potentials resulted in the formation of light absorbing Magneli phases in the incorporated TiO_2[9]. However, in the present study no evidence of un-anodised Al was found during the microstructural investigations as shown in Figure 3 and Figure 4.

The thickness and frequency dependence of reflectance values (see Figure 5 and Figure 7) can also be explained by the formation of light absorbing Magneli phases in the incorporated TiO_2. The anodising time for obtaining higher anodic layer thickness increases gradually with required thickness. This results in longer exposure of the TiO_2 particles in the anodic layer to the sulphuric acid anodising electrolyte. It is known, both from the manufacturing of TiO_2 and also from thermodynamic calculations [30] that TiO_2 dissolves in sulphuric acid to form Titanyl Sulphate ($TiOSO_4$(aq.)). Aqueous titanyl sulphate in the presence of reducing agents like Al, results in reduction of Ti^{4+} to Ti^{3+}, showing a deep blue colour corresponding to light absorbing Magneli phases [31][32]. The higher reflectance values observed with increasing anodising frequency and increased anodic cycle potential can also be explained in a similar fashion due to the reduced anodising time for a given anodic layer thickness (see Figure 2 (a)).

3.4 Hardness measurements

Figure 8

The micro-Vickers hardness values of the high frequency anodised surfaces (see Figure 8) show a decreasing trend with increasing anodic layer thickness. With increasing anodising frequency, the hardness values show an increase initially up to a frequency of 2 kHz, but appear to be slightly lower at 10 kHz for all duty cycles (Figure 9 (a)). The hardness values show a slightly increasing trend with increasing duty cycle for all the anodising frequencies investigated for +10 V and +20 V anodic cycle potential values (see Figure 9 (b)). The reduction in hardness with increase in thickness is due to the dissolution of the pore inner walls and subsequent weakening of the anodised layer formed in the initial stages of anodising [33]. Higher anodised layer thicknesses obtained by longer anodising times result in the 'powdering' of the anodised layer due to chemical dissolution by the sulphuric acid electrolyte [34][35]. Similarly, higher anodising times required for obtaining a specific anodic layer thickness at lower anodising frequencies also result in lower mechanical hardness of the anodised surfaces. Increasing the duty cycle slightly improves the growth rate of the anodic films and reduces the 'off' time that contributes to dissolution and mechanical weakening of the anodised surface. Thus higher mechanical hardness is expected at higher duty cycles. However, duty cycle values reaching DC conditions (approx. 80 % - 90 %) result in higher heat generation and lower heat dissipation causing increased dissolution due to temperature effects and hence lower the mechanical hardness [21].

Overall, it was observed that the higher anodic cycle potentials give better growth rates for high frequency anodising of the Al-TiO_2 surface composites. Similar behaviour is also observed

with increasing pulse frequency. Surface reflectance as well as hardness of the anodised surfaces also showed an improving trend with increasing the anodic cycle potential and pulse frequency.

Figure 9

4. Conclusions

- High frequency pulse reverse pulse anodising was shown to be an effective technique for obtaining high reflectance anodised surfaces over FSP surface composites of Al-TiO_2.
- The growth rate of anodic layer increases with an increase in the anodic cycle voltage and anodising frequency, but it is almost independent of the duty cycle at +10 V and slightly increases at +20 V anodic cycle potential.
- The total optical reflectance of the anodised surfaces depends on the anodic cycle voltage, frequency, and the duty cycle. In general, increasing the anodic cycle voltage and frequency leads to an increase in the total reflectance.
- High frequency anodising of the samples with voltage amplitude of -2 V to +10 V is accompanied by pore branching and allows complete oxidation of Al in the regions below the embedded TiO_2 particles. At the higher positive cycle voltage (+20 V), all of the embedded particles are disintegrated during the anodising.
- Micro-hardness of the anodised surfaces increases with anodising frequency and duty cycle, and reduces with the anodic layer thickness.

Acknowledgements

The authors would like to thank the Danish National Advanced Technology Foundation for their financial support in the ODAAS project and all the involved project partners. Dr. Jørgen Schou is acknowledged for help with reflectance spectroscopy measurements. Aude Simar acknowledges the financial support from the Interuniversity Attraction Poles Program from the Belgian State through the Belgian Policy agency; contract IAP7/21 “INTEMATE”.

References

[1] P.G. Sheasby, R. Pinner, The Surface Treatment and Finishing of Aluminium and Its Alloys, Volume 1, 6th ed., ASM International; Finishing Publications, 2001.

[2] P.G. Sheasby, R. Pinner, The Surface Treatment and Finishing of Aluminium and Its Alloys, Volume 2, 6th ed., ASM International; Finishing Publications, 2001.

[3] C.A. Grubbs, Anodizing of Aluminum, Met. Finish. 105 (2007) 397–412. doi:10.1016/S0026-0576(07)80359-X.

[4] G.E. Thompson, G.C. Wood, Porous anodic film formation on aluminium, Nature. 290 (1981) 230–232. doi:doi:10.1038/290230a0.

[5] S. Canulescu, K. Rechendorff, C.N. Borca, N.C. Jones, K. Bordo, J. Schou, et al., Band gap structure modification of amorphous anodic Al oxide film by Ti-alloying, Appl. Phys. Lett. 104 (2014) 121910. doi:10.1063/1.4866901.

[6] C. Siva Kumar, S.M. Mayanna, K.N. Mahendra, A.K. Sharma, R. Uma Rani, Studies on white anodizing on aluminum alloy for space applications, Appl. Surf. Sci. 151 (1999) 280–286. doi:10.1016/S0169-4332(99)00290-1.

[7] C. Siva Kumar, A.K. Sharma, K.N. Mahendra, S.M. Mayanna, Studies on anodic oxide coating with low absorptance and high emittance on aluminum alloy 2024, Sol. Energy Mater. Sol. Cells. 60 (2000) 51–57. doi:10.1016/S0927-0248(99)00062-8.

[8] V.C. Gudla, F. Jensen, S. Canulescu, A. Simar, R. Ambat, Friction Stir Processed Al-Metal Oxide Surface Composites: Anodising and Optical Appearance, in: T.S. Sudarshan, P. Vuoristo, H. Koivuluoto (Eds.), Surf. Modif. Technol. XXVIII, ValarDocs, Tampere, Finland, 2014: pp. 375–384.

[9] V.C. Gudla, F. Jensen, A. Simar, R. Shabadi, R. Ambat, Friction stir processed Al–TiO2 surface composites: Anodising behaviour and optical appearance, Appl. Surf. Sci. 324 (2015) 554–562. doi:http://dx.doi.org/10.1016/j.apsusc.2014.10.151.

[10] V.C. Gudla, S. Canulescu, R. Shabadi, K. Rechendorff, J. Schou, R. Ambat, Anodization and Optical Appearance of Sputter Deposited Al-Zr Coatings, in: J. Grandfield, TMS (Eds.), Light Met. 2014, John Wiley & Sons, Inc., 2014: pp. 369–373. doi:10.1002/9781118888438.ch63.

[11] V.C. Gudla, S. Canulescu, R. Shabadi, K. Rechendorff, K. Dirscherl, R. Ambat, Structure of anodized Al-Zr sputter deposited coatings and effect on optical appearance, Appl. Surf. Sci. 317 (2014) 1113–1124. doi:http://dx.doi.org/10.1016/j.apsusc.2014.09.037.

[12] M. Aggerbeck, A. Junker-Holst, D.V. Nielsen, V.C. Gudla, R. Ambat, Anodisation of sputter deposited aluminium-titanium coatings: Effect of microstructure on optical characteristics, Surf. Coatings Technol. 254 (2014) 138–144. doi:10.1016/j.surfcoat.2014.05.073.

[13] T. Yamamoto, H. Tanaka, M. Fujita, H. Asoh, S. Ono, Effect of high-frequency switching electrolysis on film thickness uniformity of anodic oxide film formed on AC8A Aluminum alloy, J. Japan Inst. Light Met. 60 (2010) 602–607. doi:10.2464/jilm.60.602.

[14] L.. Fratila-Apachitei, F.D. Tichelaar, G.E. Thompson, H. Terryn, P. Skeldon, J. Duszczyk, et al., A transmission electron microscopy study of hard anodic oxide layers on AlSi(Cu) alloys, Electrochim. Acta. 49 (2004) 3169–3177. doi:10.1016/j.electacta.2004.02.030.

[15] M. Fujita, H. Tanaka, H. Muramatsu, T. Yamamoto, H. Asoh, S. Ono, Effect of High Frequency Switching Electrolysis on Structure of Anodic Oxide Film Formed on Aluminum Alloy, J. Surf. Finish. Soc. Japan. 62 (2011) 346–350.

[16] H.S. Arora, H. Singh, B.K. Dhindaw, Composite fabrication using friction stir processing - A review, Int. J. Adv. Manuf. Technol. 61 (2012) 1043–1055. doi:10.1007/s00170-011-3758-8.

[17] R.S. Mishra, Z.Y. Ma, I. Charit, Friction stir processing: A novel technique for fabrication of surface composite, Mater. Sci. Eng. A. 341 (2003) 307–310. doi:10.1016/S0921-5093(02)00199-5.

[18] E.D. Palik, Chapter 2 - Refractive Index, Handbook of Optical Constanst of Solids, in: Handb. Opt. Constants Solids, Academic Press, Burlington, 1997: pp. 5–114. doi:http://dx.doi.org/10.1016/B978-012544415-6.50149-7.

[19] V.C. Gudla, V.E. Johansen, S. Canulescu, J. Schou, R. Ambat, Simulation of Reflectance from White Anodised Aluminium Surfaces Using Polyurethane-TiO2 Composite Coatings, J. Mater. Sci. 50 (2015) 4565–4575. doi:DOI: 10.1007/s10853-015-9005-1.

[20] D. Kanagaraj, V. Raj, S. Vincent, S.V. Iyer, Effect of Pulse Frequency on Pulse Anodising of AA1100 Aluminium Alloy in Sulphamic Acid, Bull. Electrochem. 17 (2001) 523–526.

[21] D. Kanagaraj, V. Raj, S. Vincent, B.P. Kumar, A.S. Kumar, S.V. Iyer, Pulse anodizing of AA1100 aluminium alloy in oxalic acid electrolyte, Bull. Electrochem. 17 (2001) 285–288.

[22] K. Yokoyama, H. Konno, H. Takahashi, M. Nagayama, Advantages of Pulse Anodizing, Plat. Surf. Finish. 69 (1982) 62–65.

[23] L. Zhang, G.E. Thompson, M. Curioni, P. Skeldon, Anodizing of Aluminum in Sulfuric Acid/Boric Acid Mixed Electrolyte, J. Electrochem. Soc. 160 (2013) C179–C184. doi:10.1149/2.032306jes.

[24] T. Ohno, K. Sarukawa, K. Tokieda, M. Matsumura, Morphology of a TiO2 photocatalyst (Degussa, P-25) consisting of anatase and rutile crystalline phases, J. Catal. 203 (2001) 82–86. doi:10.1006/jcat.2001.3316.

[25] E. Kowalska, O.O.P. Mahaney, R. Abe, B. Ohtani, Visible-light-induced photocatalysis through surface plasmon excitation of gold on titania surfaces, Phys. Chem. Chem. Phys. 12 (2010) 2344–2355. doi:10.1039/B917399D.

[26] V.C. Gudla, F. Jensen, K. Bordo, A. Simar, R. Ambat, Effect of High Frequency Pulsing on the Interfacial Structure of Anodized Aluminium-TiO2, J. Electrochem. Soc. 162 (2015) C303–C310. doi:10.1149/2.0311507jes.

[27] M. Saito, Unoxidized Aluminum Particles in Anodic Alumina Films, J. Electrochem. Soc. 140 (1993) 1907. doi:10.1149/1.2220737.

[28] A.E. Hultquist, On the Nature of Burned Anodic Coatings, J. Electrochem. Soc. 111 (1964) 1302. doi:10.1149/1.2425989.

[29] R. Chang, W.F. Hall, On the correlation between optical properties and the chemical /metallurgical constitution of multi-phase thin films, Thin Solid Films. 46 (1977) L5–L8. doi:10.1016/0040-6090(77)90068-2.

[30] OutoKumpu, HSC Chemistry, (2002).

[31] M. Li, W. Hebenstreit, U. Diebold, A.M. Tyryshkin, M.K. Bowman, G.G. Dunham, et al., The influence of the bulk reduction state on the surface structure and morphology of rutile TiO2(110) single crystals, J. Phys. Chem. B. 104 (2000) 4944–4950. doi:Doi 10.1021/Jp9943272.

[32] U. Diebold, M. Li, O. Dulub, E.L.D. Hebenstreit, W. Hebenstreit, The relationship between bulk and surface properties of rutile TiO2 (110), Surf. Rev. Lett. 07 (2000) 613–617. doi:10.1142/S0218625X0000052X.

[33] R.C. Furneaux, W.R. Rigby, B.G. Carter, Mechanisms of Short-Term Superficial Weathering of Anodized Aluminium, Proc. - INTERFINISH 84, 11th World Congr. Met. Finish. (1984) 376–384.

[34] M. Nagayama, K. Tamura, Dissolution of the anodic oxide film on aluminium in a sulphuric acid solution, Electrochim. Acta. 12 (1967) 1097–1107. doi:http://dx.doi.org/10.1016/0013-4686(67)80105-1.

[35] M. Nagayama, K. Tamura, H. Takahashi, Dissolution of porous anodic oxide films on Al in (COOH)2 solutions, Corros. Sci. 10 (1970) 617–627. doi:http://dx.doi.org/10.1016/S0010-938X(70)80055-5.

List of Figure Captions

Figure 1: Voltage profile used for high frequency pulse reverse pulse anodising (PRPA) of FSP Al-TiO_2 surface composites.

Figure 2: Rate of the anodic film growth as a function of: (a) pulse frequency and (b) duty cycle.

Figure 3: Cross section of anodic layer obtained at anodic cycle potential of + 10 V, 2 kHz, 50% duty cycle: SEM-BSE images showing (a) TiO_2 particles incorporated into anodic layer, (b) difference in contrast within TiO_2 particles, and bright field TEM images showing: (c) porous nature of the TiO_2 particles in anodic layer and (d) anodic pore branching at TiO_2 particle locations.

Figure 4: Cross section of anodic layer obtained at anodic cycle potential of + 20 V, 2 kHz, 50% duty cycle: SEM-BSE images showing (a), (b) TiO_2 particles incorporated into anodic layer with difference in contrast between TiO_2 particles in Al substrate and anodic layer, and bright field TEM images showing: (c) porous nature of the TiO_2 particles and pore branching in anodic layer and (d) porosity of TiO_2 particles.

Figure 5: Total and diffuse reflectance of the high frequency anodised surfaces as a function of the anodic layer thickness (T- Total reflectance, D – Diffuse reflectance).

Figure 6: Optical reflectance of high frequency anodised FSP-treated samples as a function of the anodic cycle voltage (T- Total reflectance, D – Diffuse reflectance).

Figure 7: Optical reflectance of high frequency anodised FSP-treated samples as a function of the pulse frequency with: (a) +10 V and (b) +20 V as the anodic cycle potential.

Figure 8: Hardness of high frequency anodised surfaces measured as a function of anodised layer thickness.

Figure 9: Hardness of high frequency anodised surfaces measured as a function of: (a) duty cycle and (b) anodising frequency

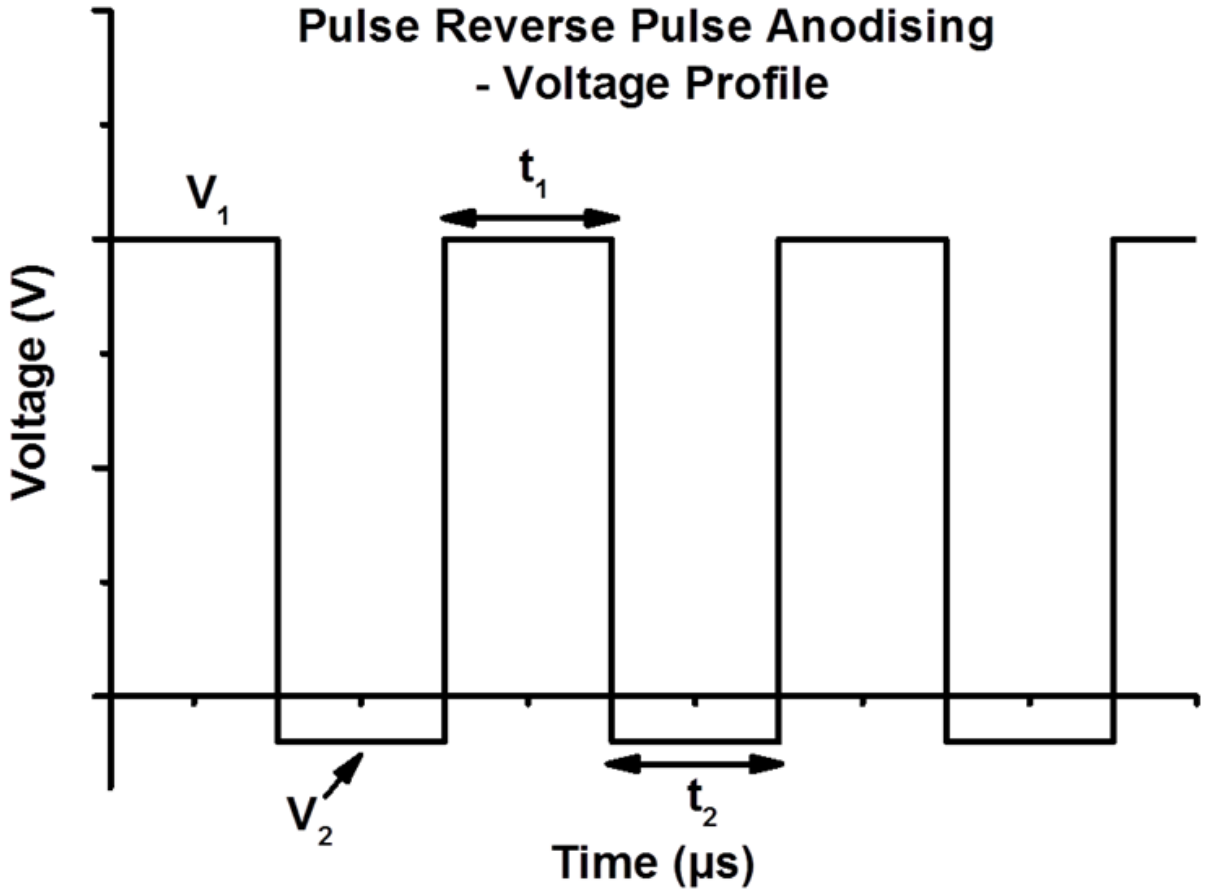

Figure 1

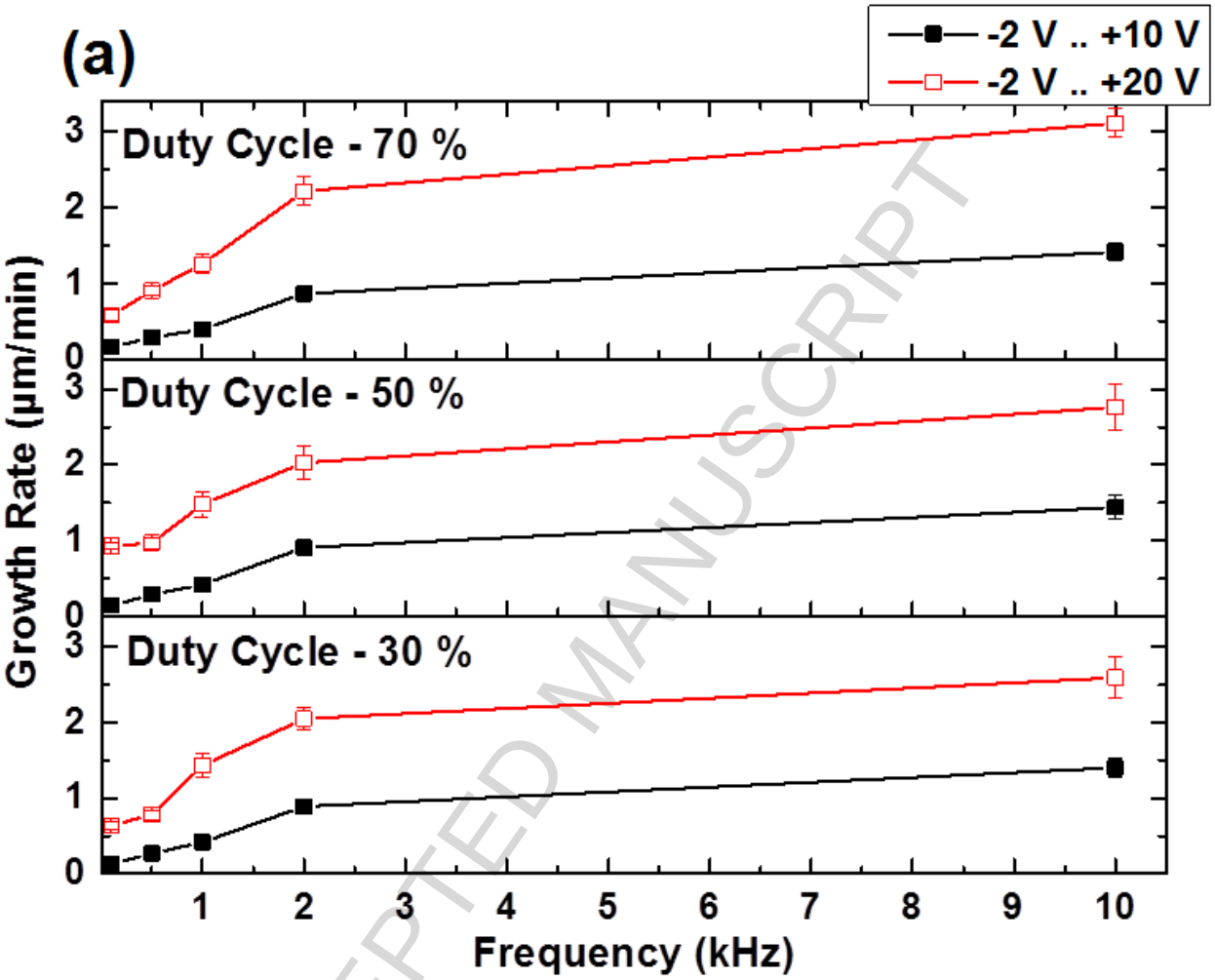

Figure 2(a)

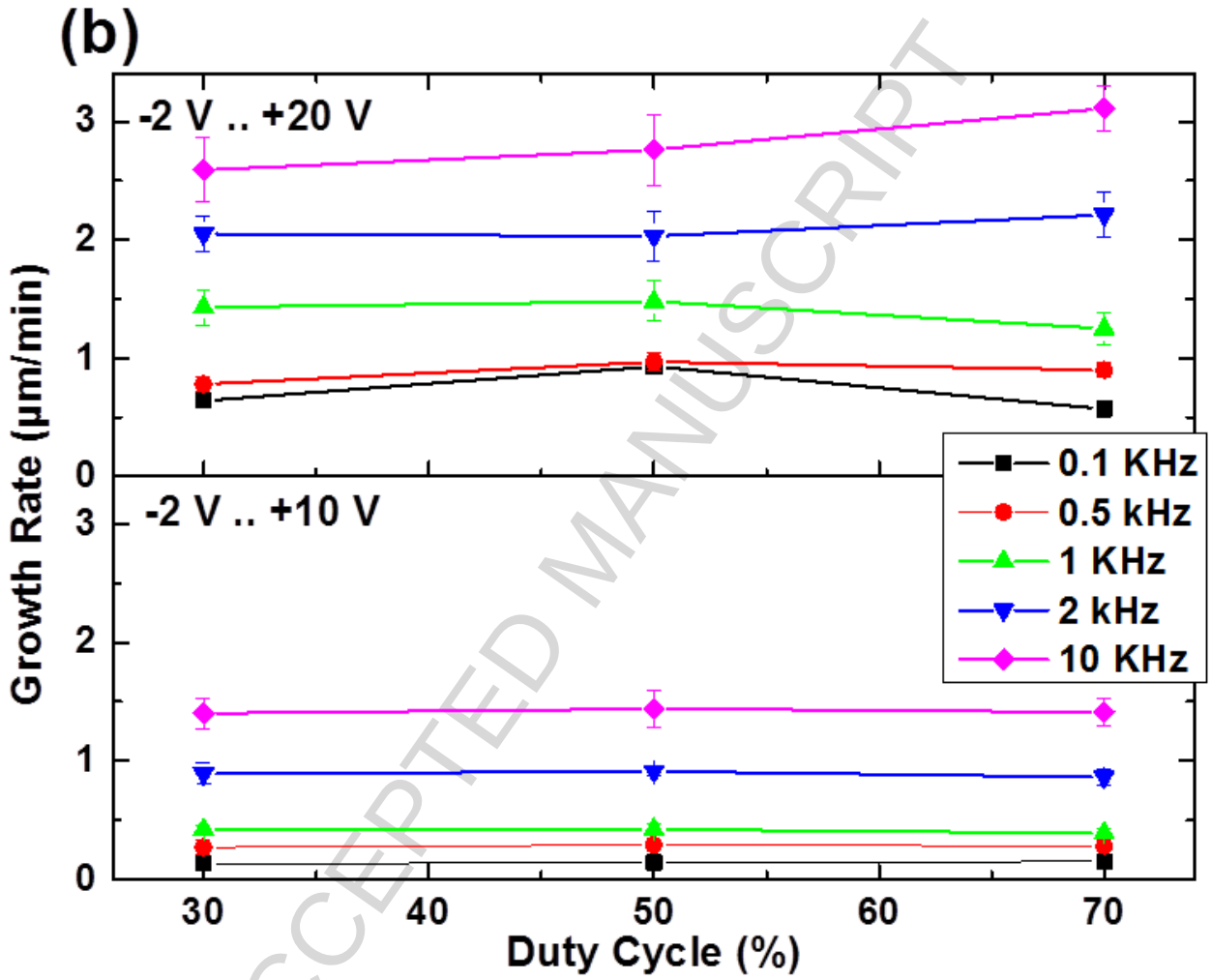

Figure 2(b)

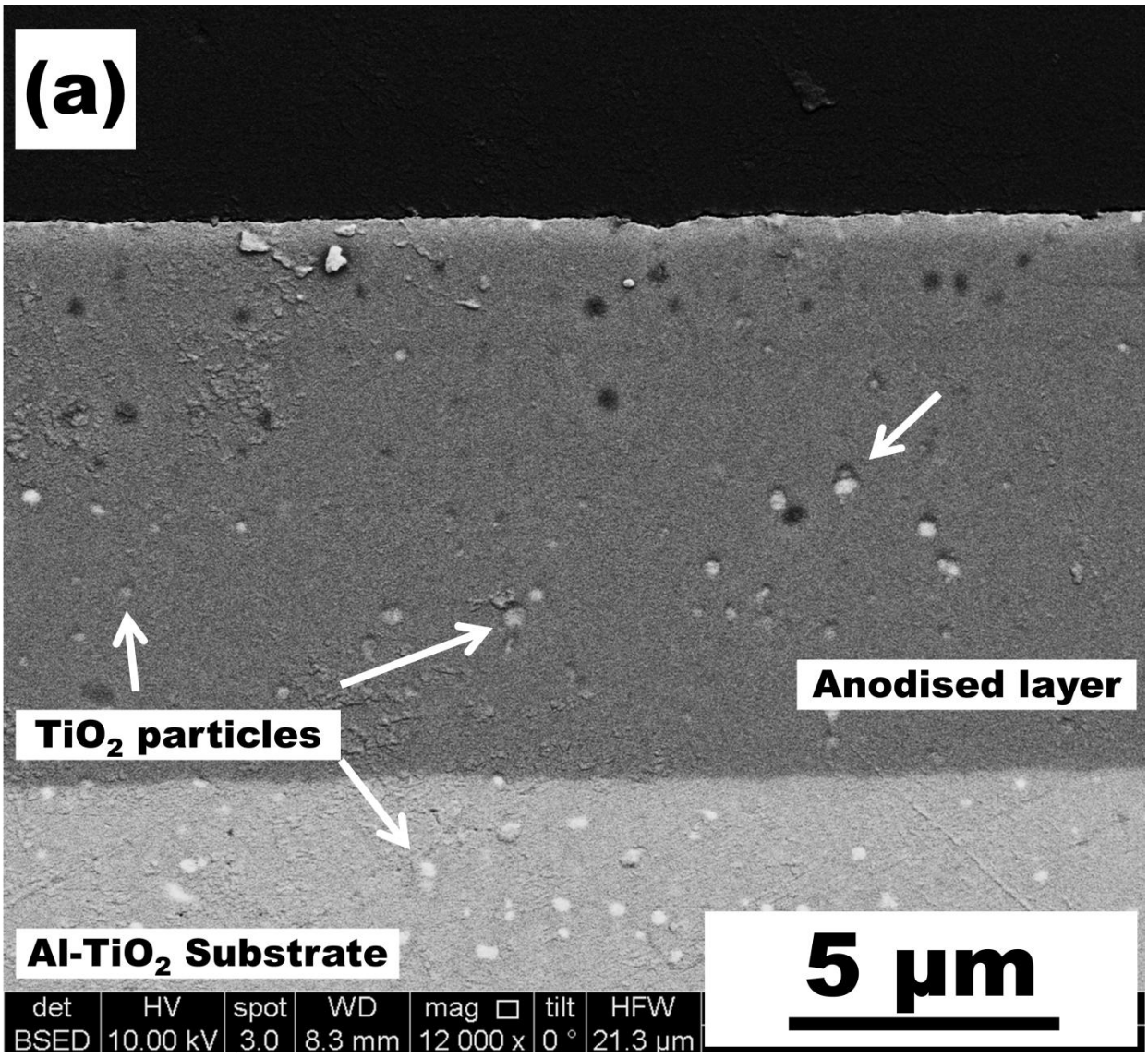

Figure 3(a)

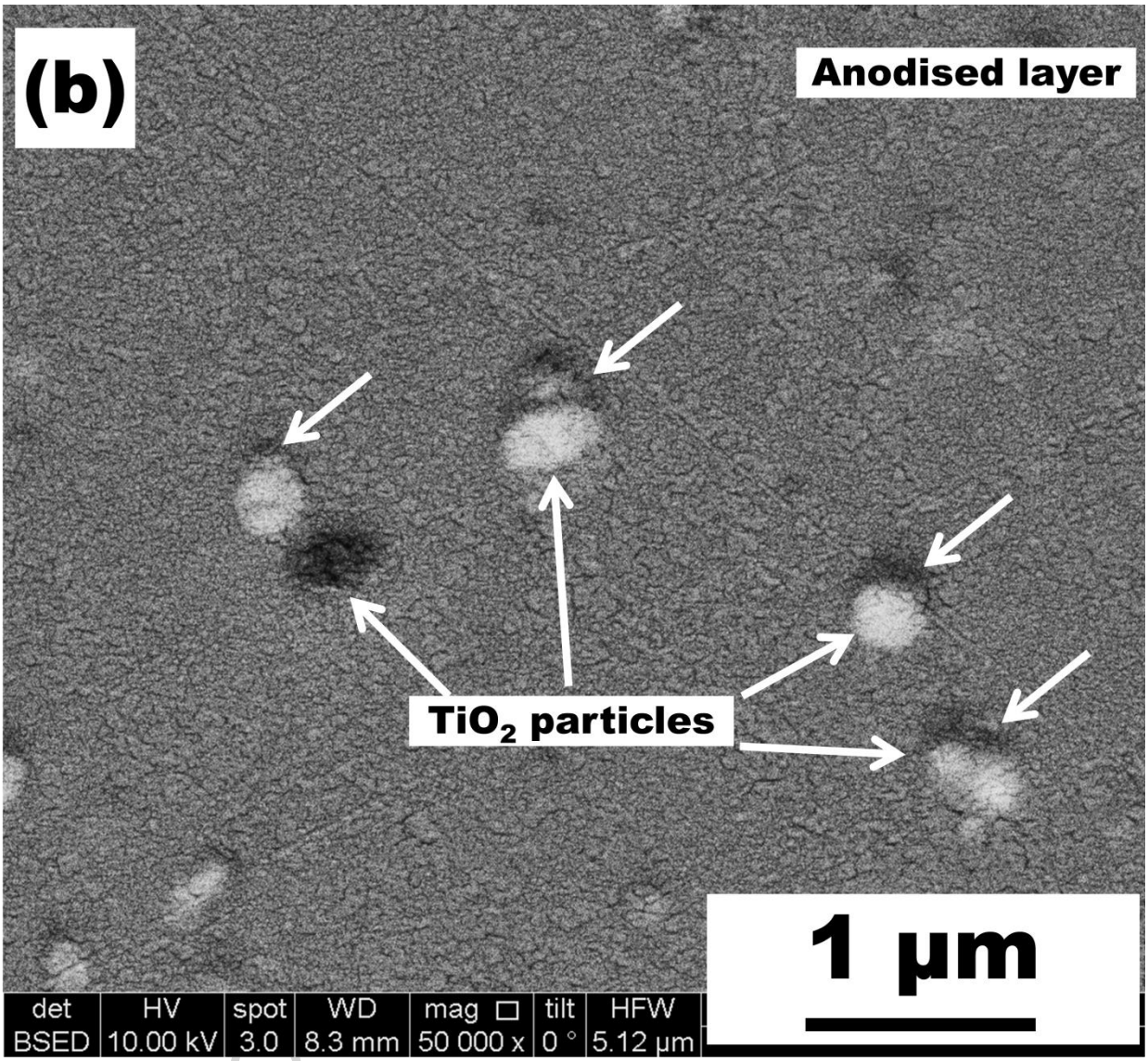

Figure 3(b)

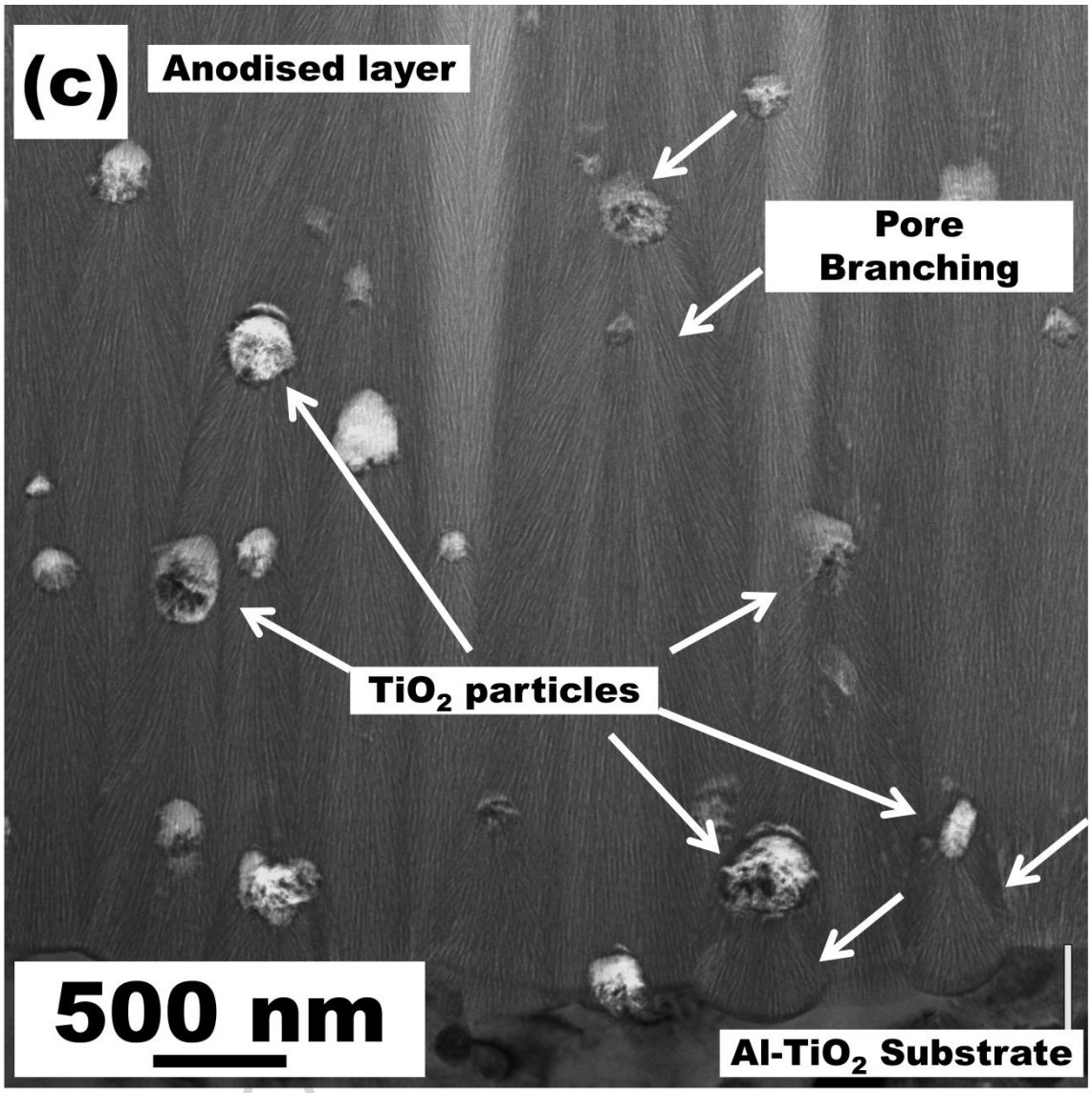

Figure 3(c)

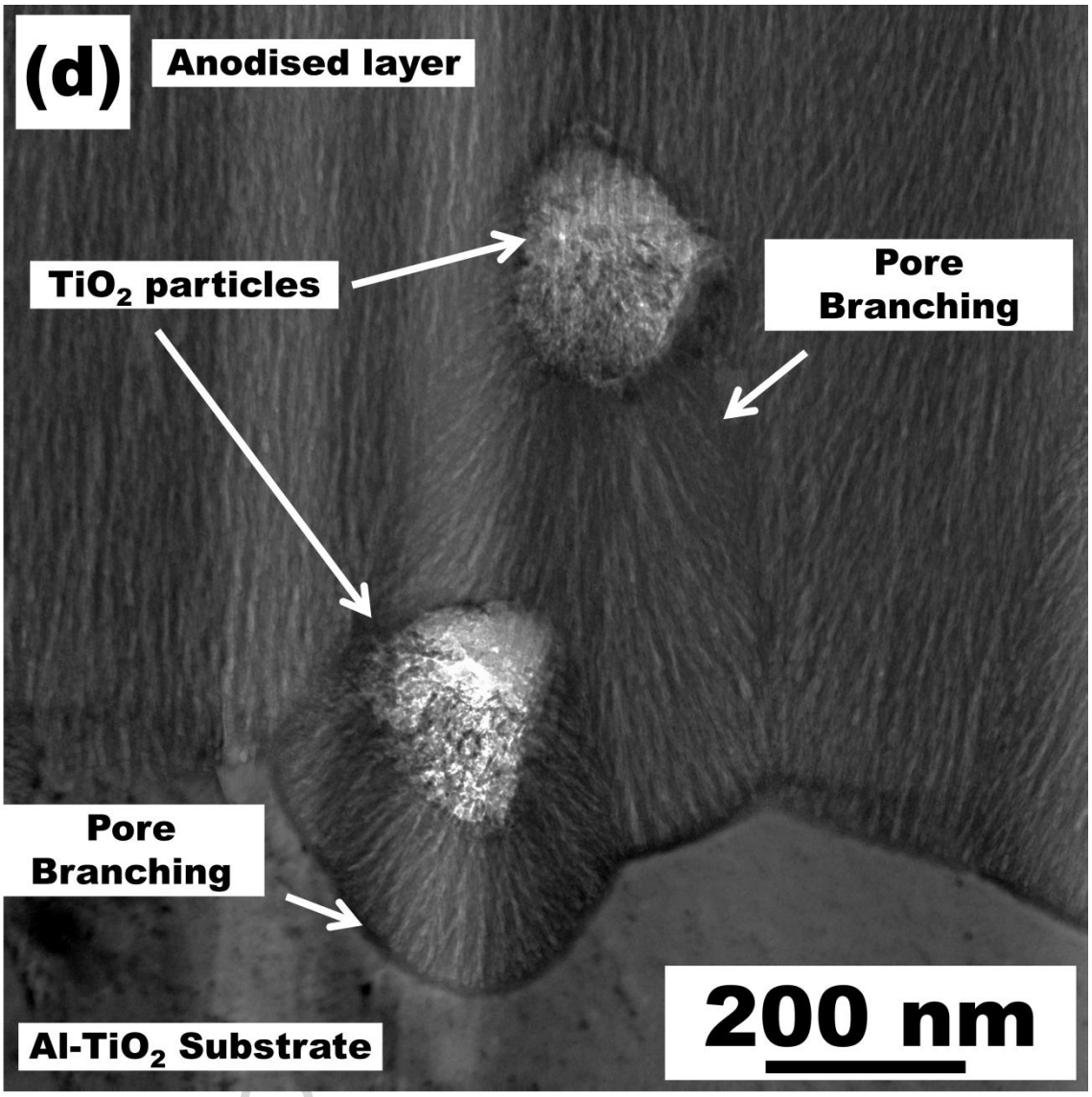

Figure 3(d)

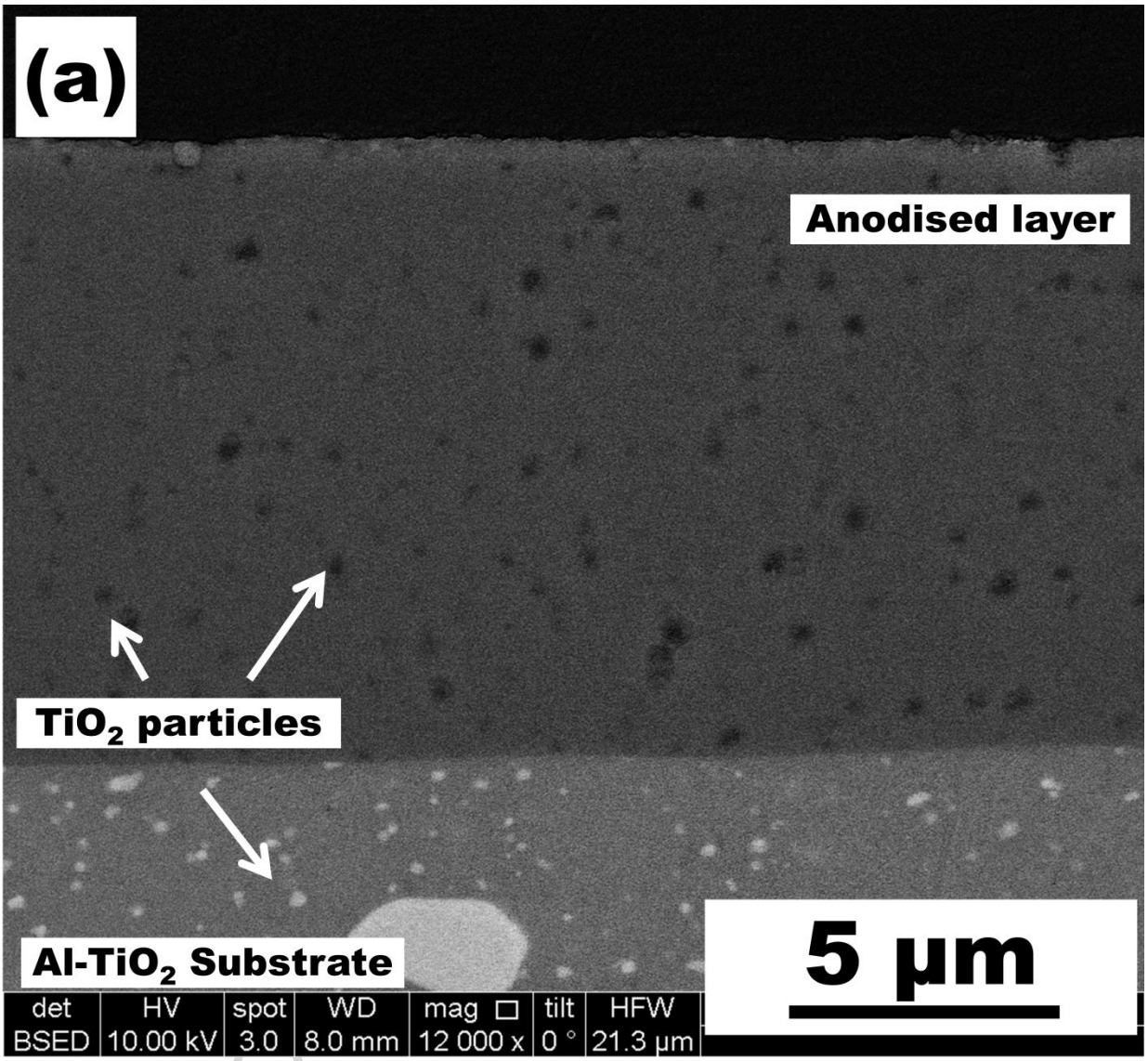

Figure 4(a)

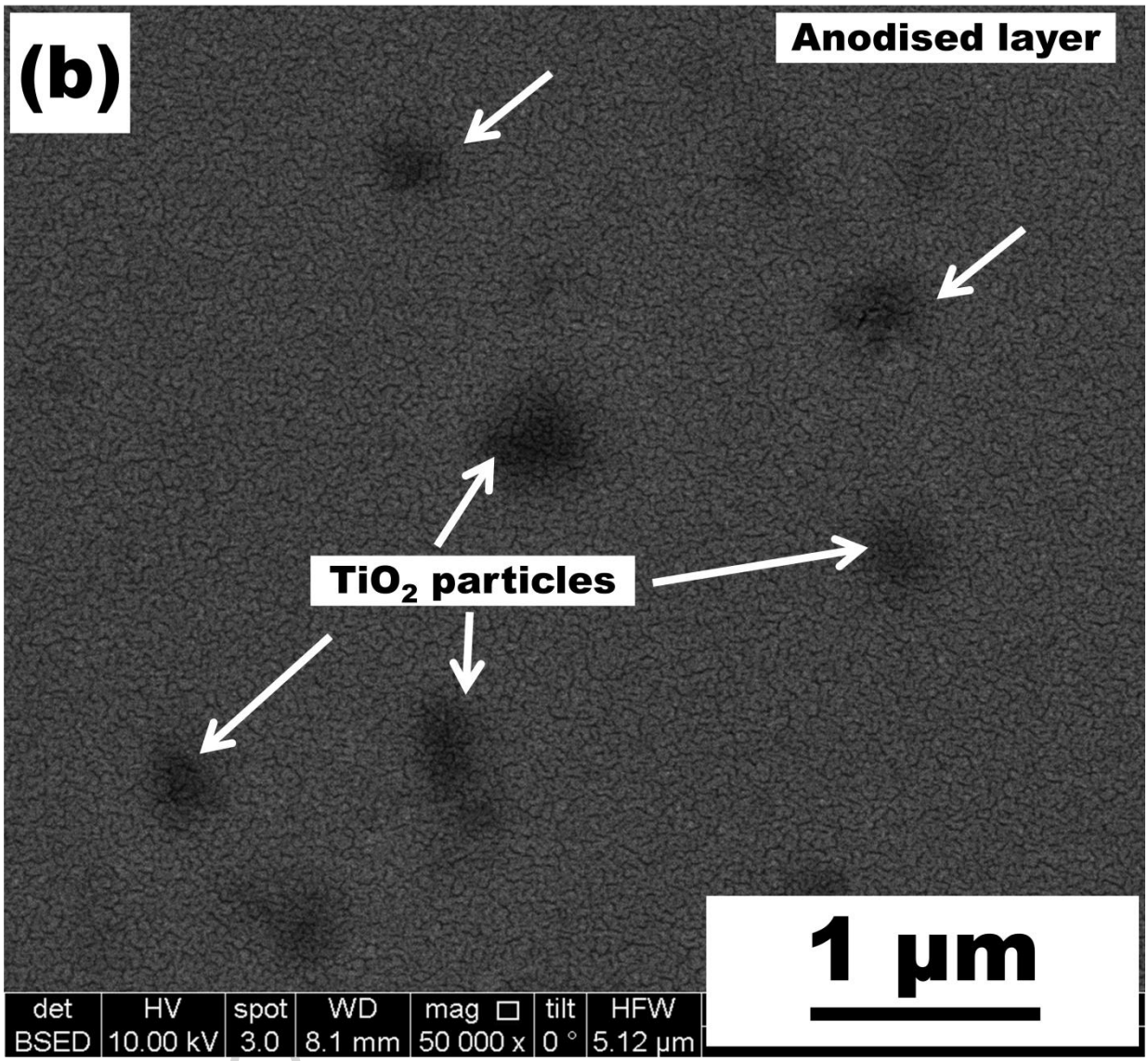

Figure 4(b)

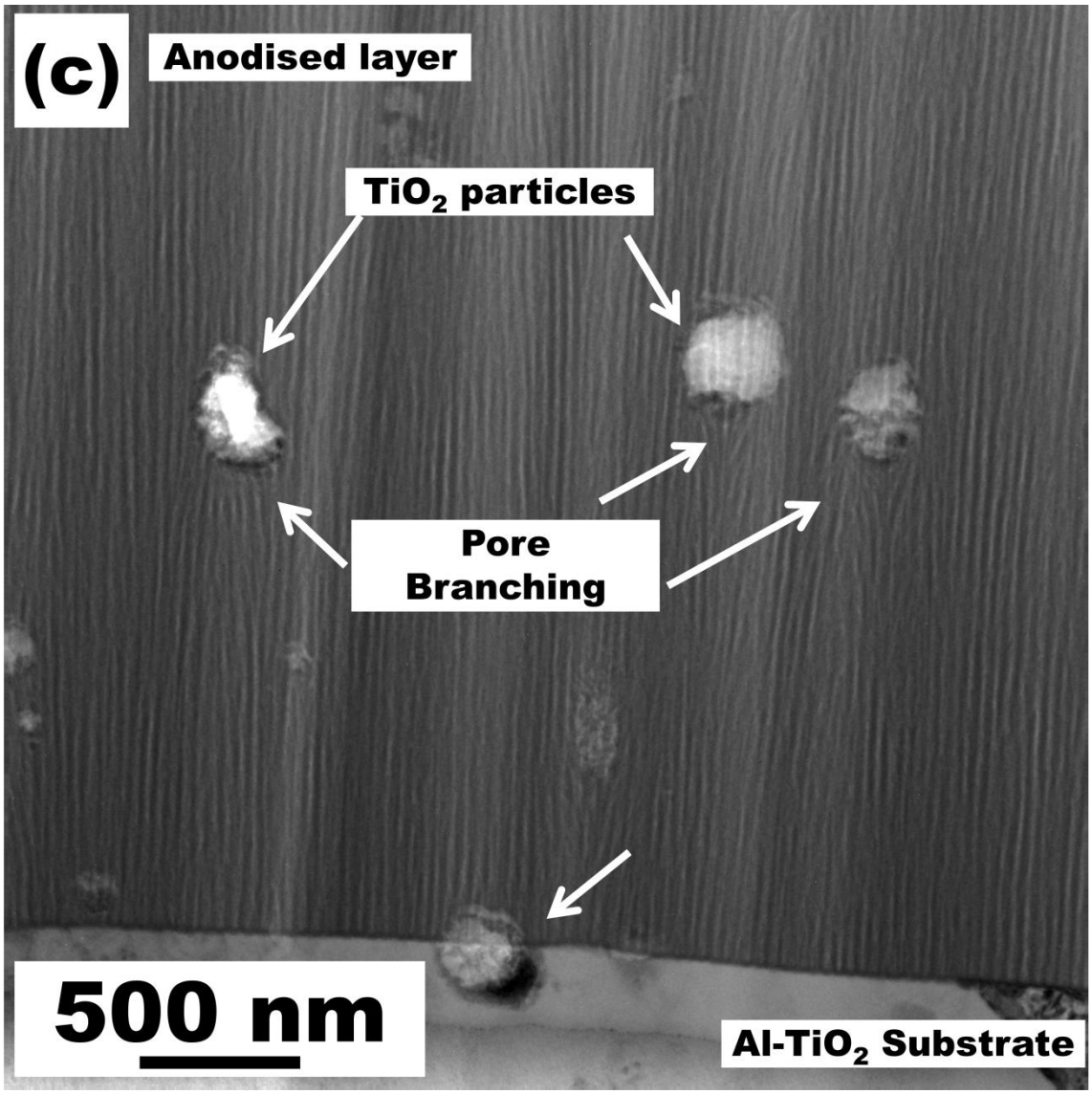

Figure 4(c)

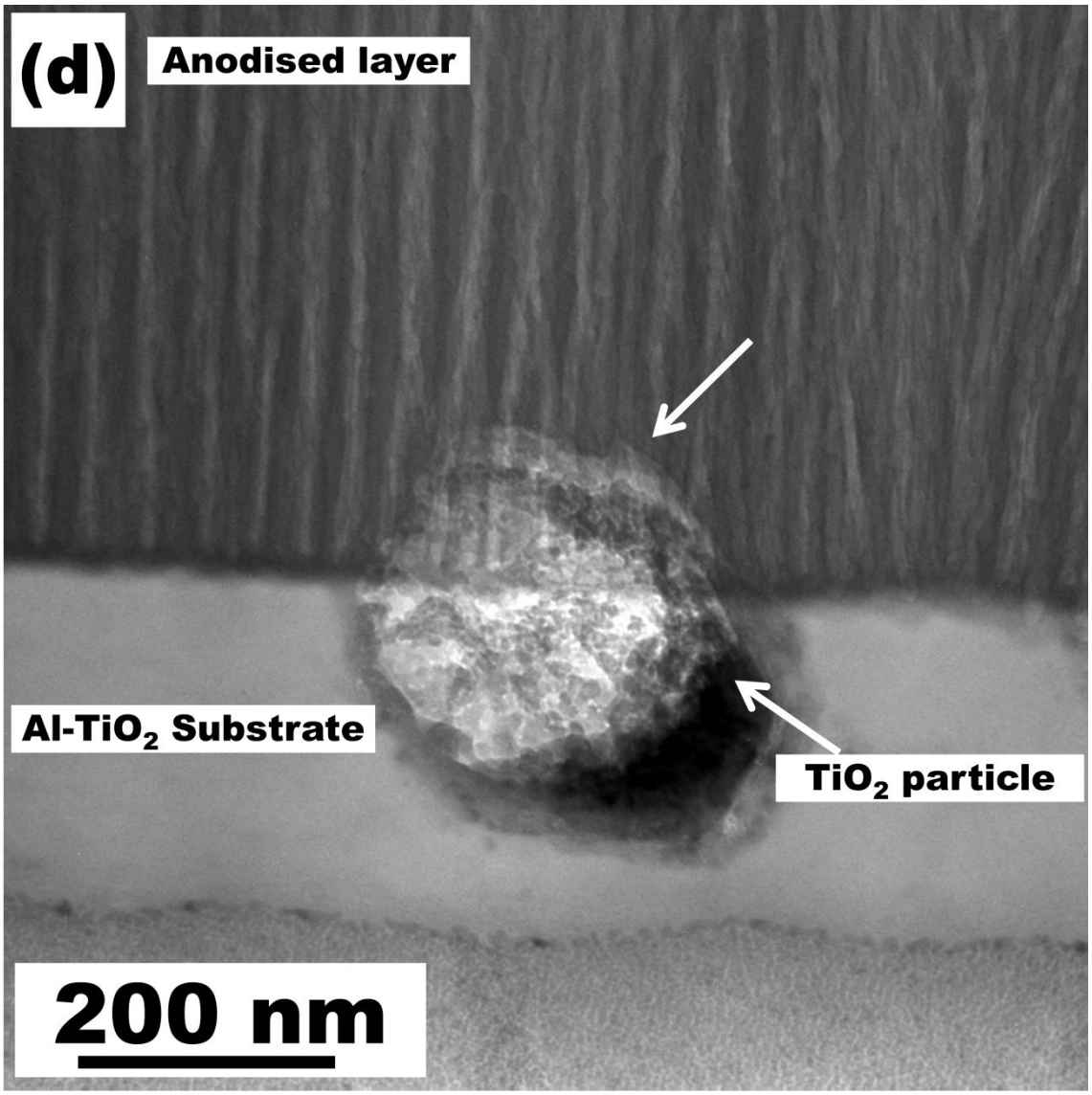

Figure 4(d)

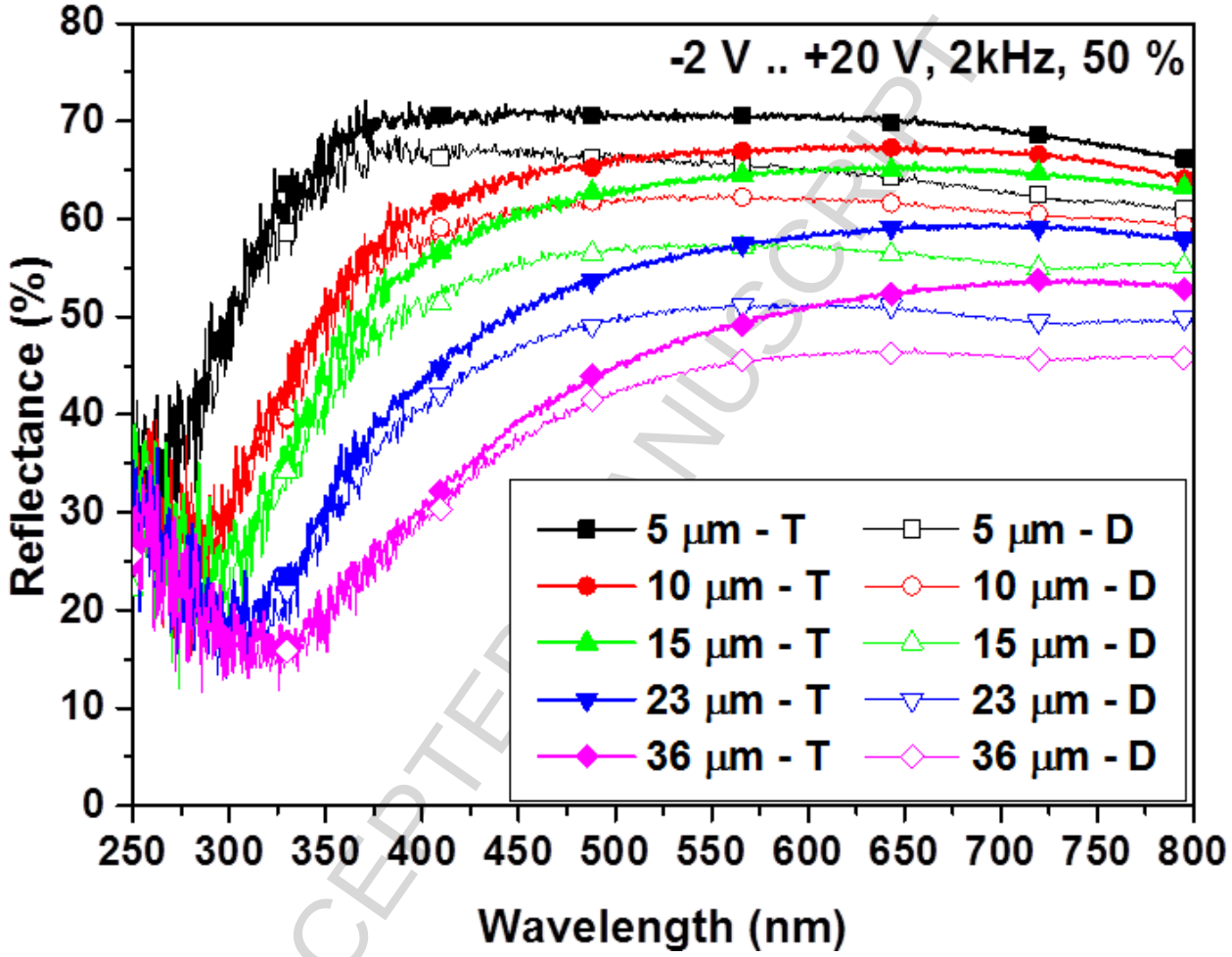

Figure 5

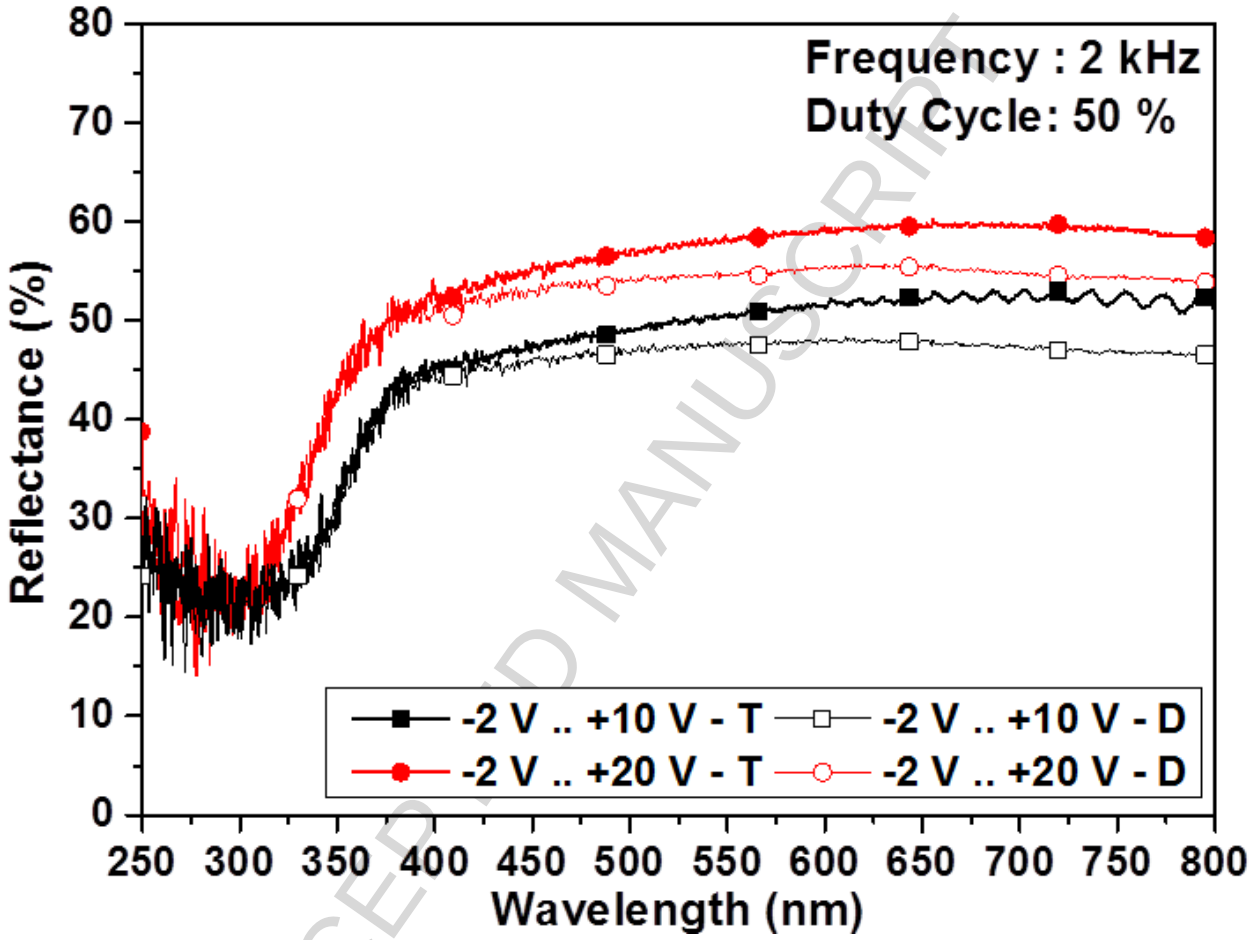

Figure 6

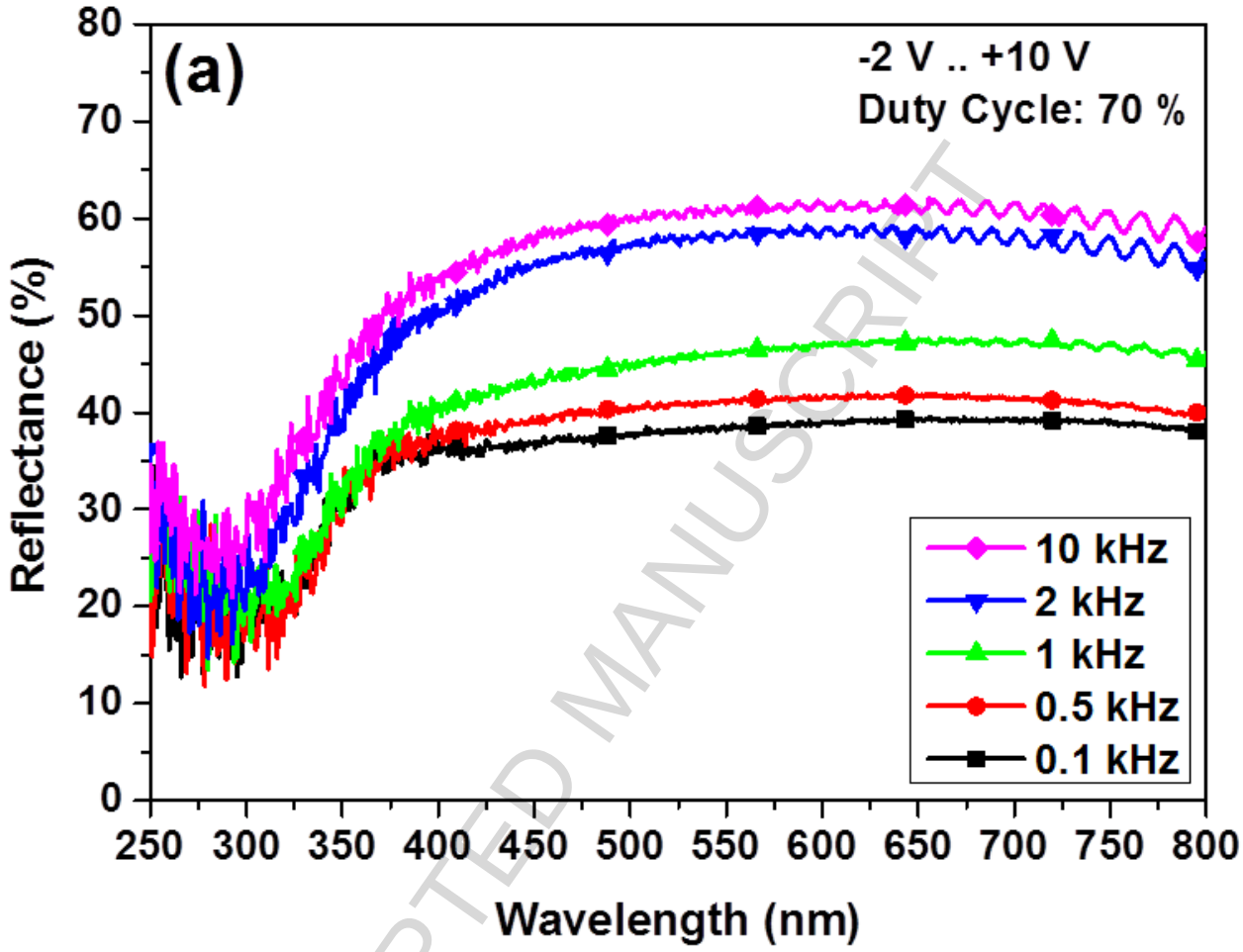

Figure 7(a)

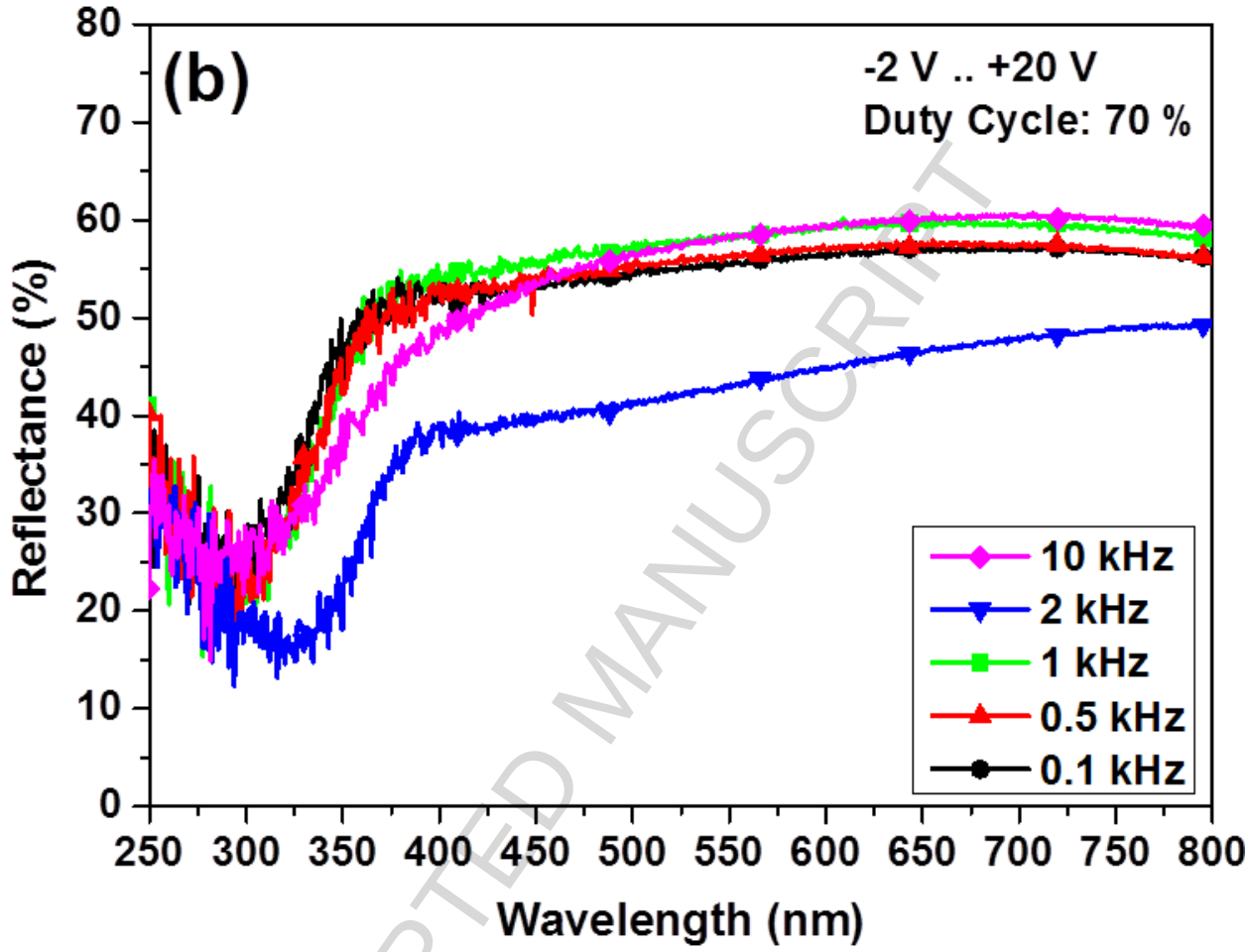

Figure 7(b)

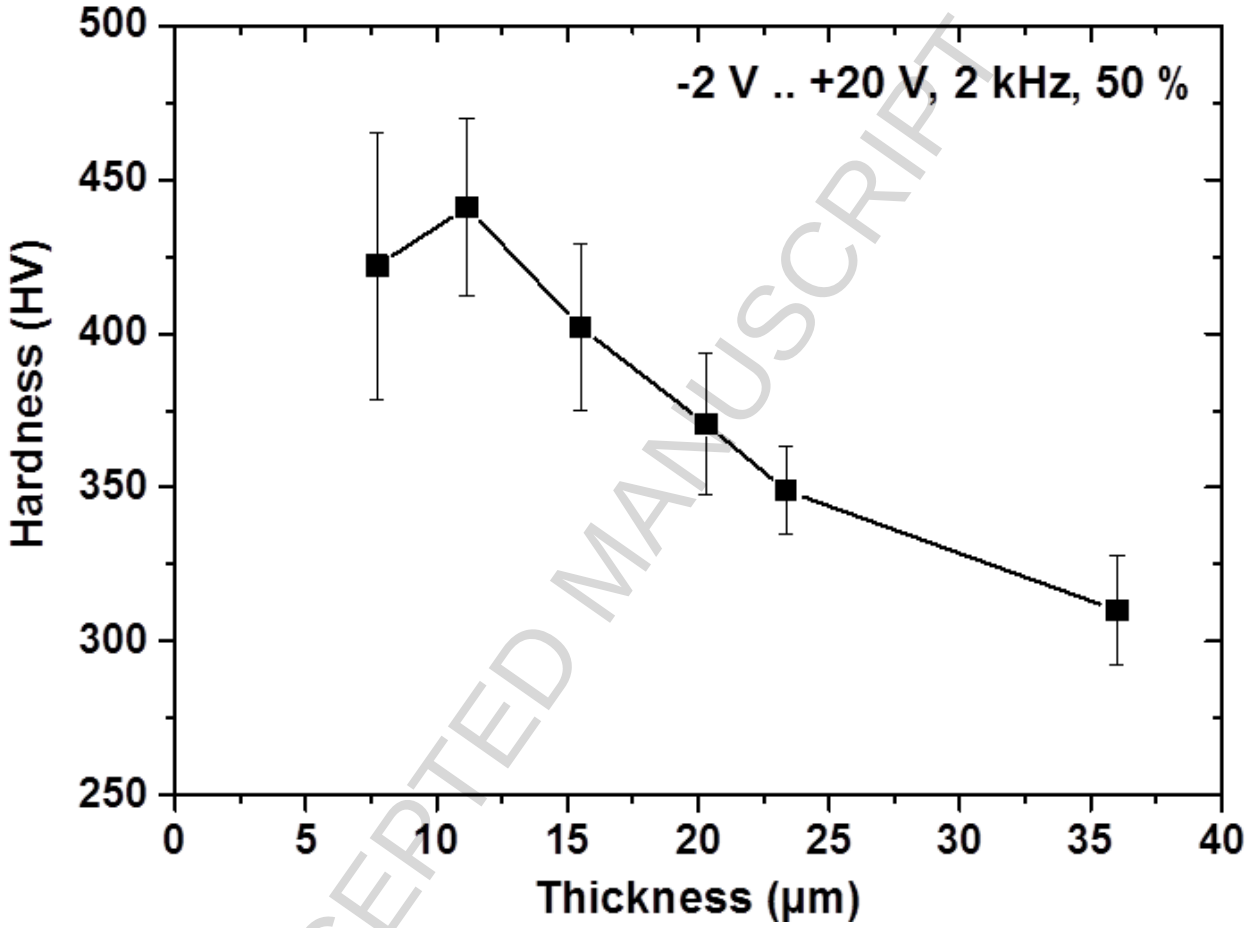

Figure 8

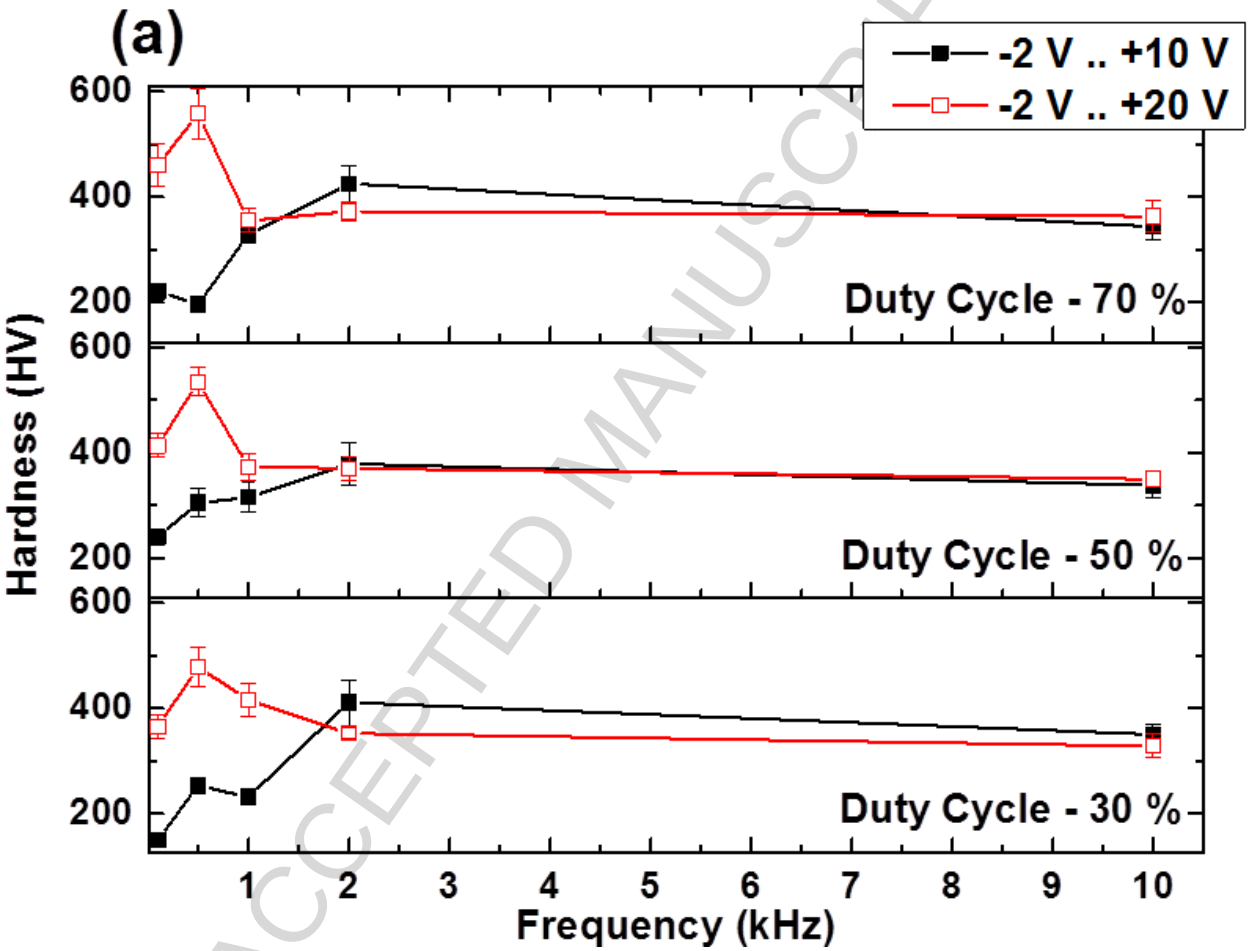

Figure 9(a)

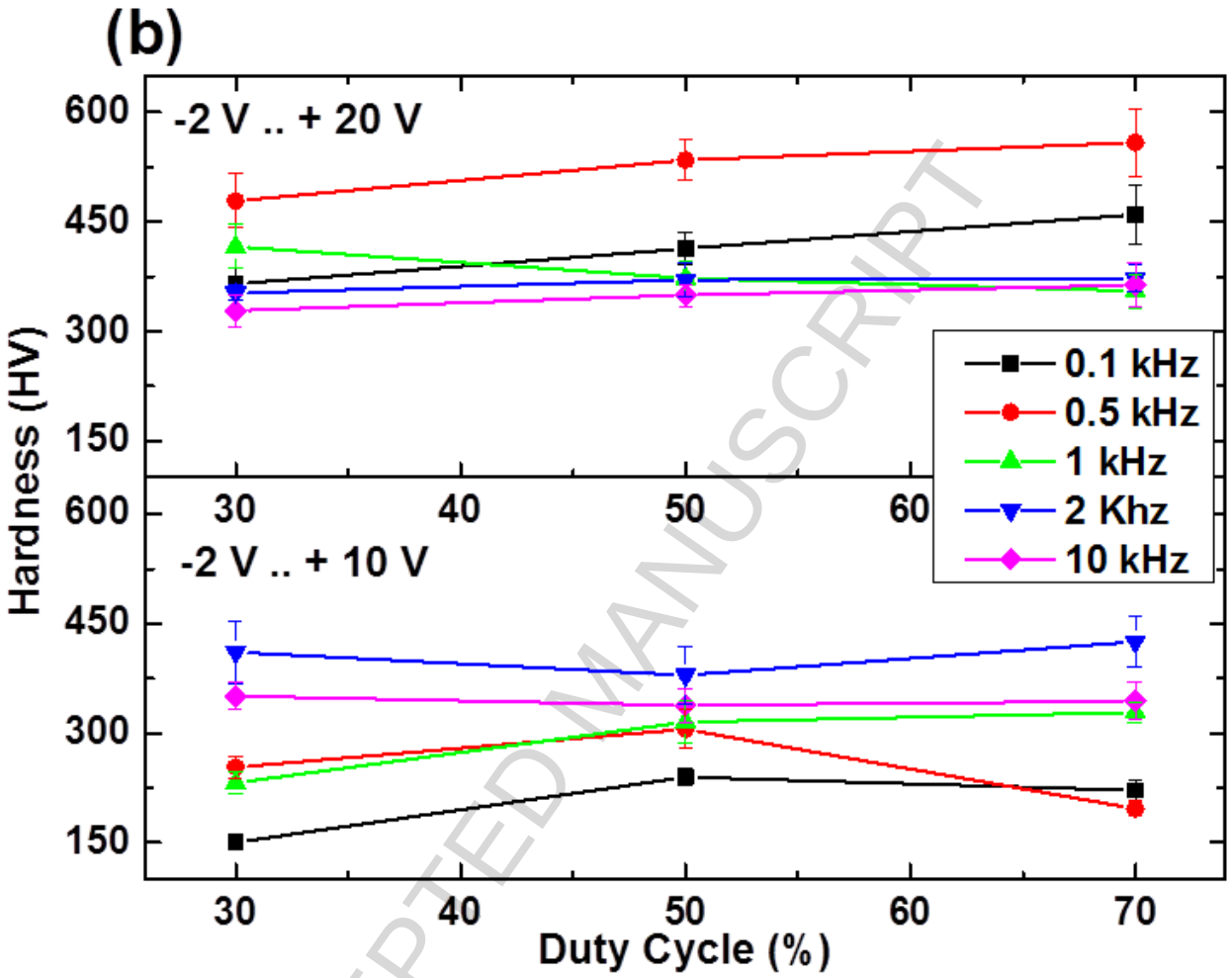

Figure 9(b)

Research Highlights

- High frequency pulse reverse pulse anodising of friction stir processed Al-TiO_2 surface composites was investigated.
- Increasing pulse frequency and anodising potential resulted in higher growth rates and increased reflectance.
- Change in pulse duty cycle during anodising showed a negligible effect on the growth rates.
- High frequency anodising shows tortuous anodic pore branching and disintegration of incorporated TiO_2 particles.
- Hardness of anodised surfaces increases with pulse frequency and duty cycle and decreases with anodic layer thickness.